

Individual voxel-based morphometry adjusting covariates in multiple system atrophy

Junya Ebina^{a,b}, Kazuhiro Hara^c, Hirohisa Watanabe^{a,d,**}, Kazuya Kawabata^{a,c},
Fumio Yamashita^e, Atsushi Kawaguchi^f, Yusuke Yoshida^c, Toshiyasu Kato^c, Aya Ogura^c,
Michihito Masuda^c, Reiko Ohdake^{a,d}, Daisuke Mori^a, Satoshi Maesawa^{a,g}, Masahisa Katsuno^c,
Osamu Kano^b, Gen Sobue^{a,*}

^a Brain and Mind Research Center, Nagoya University, Aichi, Japan

^b Division of Neurology, Department of Internal Medicine, Toho University Graduate School of Medicine, Tokyo, Japan

^c Department of Neurology, Nagoya University Graduate School of Medicine, Aichi, Japan

^d Department of Neurology, Fujita Health University School of Medicine, Aichi, Japan

^e Division of Ultrahigh-Field MRI, Institute for Biomedical Sciences, Iwate Medical University, Iwate, Japan

^f Education and Research Center for Community Medicine, Faculty of Medicine, Saga University, Saga, Japan

^g Department of Neurosurgery, Nagoya University Graduate School of Medicine, Aichi, Japan

ARTICLE INFO

Keywords:

Multiple system atrophy
Parkinson's disease
Magnetic resonance imaging
Individual voxel-based morphometry adjusting covariates
Differential diagnosis

ABSTRACT

Introduction: This study aimed to evaluate whether novel individual voxel-based morphometry adjusting covariates (iVAC), such as age, sex, and total intracranial volume, could increase the accuracy of a diagnosis of multiple system atrophy (MSA) and enable the differentiation of MSA from Parkinson's disease (PD).

Methods: We included 53 MSA patients (MSA-C: 33, MSA-P: 20), 53 PD patients, and 189 healthy controls in this study. All participants underwent high-resolution T1-weighted imaging (WI) and T2-WI with a 3.0-T MRI scanner. We evaluated the occurrence of significant atrophic findings in the pons/middle cerebellar peduncle (MCP) and putamen on iVAC and compared these findings with characteristic changes on T2-WI.

Results: On iVAC, abnormal findings were observed in the pons/MCP of 96.2% of MSA patients and in the putamen of 80% of MSA patients; however, on T2-WI, they were both observed at a frequency of 60.4% in MSA patients. On iVAC, all but one MSA-P patient (98.1%) showed significant atrophic changes in the pons/MCP or putamen. By contrast, 69.8% of patients with MSA showed abnormal signal changes in the pons/MCP or putamen on T2-WI. iVAC yielded 95.0% sensitivity and 96.2% specificity for differentiating MSA-P from PD.

Conclusion: iVAC enabled us to recognize the morphological characteristics of MSA visually and with high accuracy compared to T2-WI, indicating that iVAC is a potential diagnostic screening tool for MSA.

1. Introduction

Multiple system atrophy (MSA) is an adult-onset progressive neurodegenerative disorder characterized by parkinsonism, cerebellar ataxia, pyramidal signs, and autonomic dysfunction [1]. However, the clinical diagnosis of MSA is challenging, especially in the early stage of the disease. Atrophic changes on conventional brain magnetic resonance imaging (MRI) of the putamen, middle cerebellar peduncle (MCP), pons, or cerebellum are additional features of possible MSA [2]. Besides, “classic” signs, including the “hot cross bun” and “putaminal rim” signs,

are also neuroradiological hallmarks of MSA [3–5]. Notwithstanding that the assessment of these atrophic changes and signs is subjective in nature, their presence is related to higher specificity, but lower sensitivity, for differentiating MSA from other disorders [2,6].

Voxel-based morphometry (VBM) techniques [7], which indicate the local concentration of brain tissue using unbiased statistical analysis, have been shown to be more sensitive to local volume reduction in patients with MSA than in those with Parkinson's disease (PD) and other related disorders [8,9]. While VBM methods usually require group comparisons [10], advanced imaging analysis algorithms have enabled

* Corresponding author. 65 Tsurumai-Cho, Showa-Ku, Nagoya, Japan.

** Corresponding author. 1-98 Dengakugakubo, Kutsukake-cho, Toyoake, Aichi, Japan.

E-mail addresses: nabe@med.nagoya-u.ac.jp (H. Watanabe), sobue@med.nagoya-u.ac.jp (G. Sobue).

<https://doi.org/10.1016/j.parkreldis.2021.07.025>

Received 4 February 2021; Received in revised form 16 July 2021; Accepted 23 July 2021

Available online 9 August 2021

1353-8020/© 2021 Elsevier Ltd. All rights reserved.

the atlas-based automatic assortment of the brain into multiple anatomic regions and can quantify regional tissue volume individually. This automated subcortical volume segmentation is highly predictive for differentiating MSA from PD [11,12]. However, clinical variables such as total intracranial volume (TIV), sex, and age at examination could independently influence VBM results [13–15].

We introduced a novel individual approach called individual VBM with adjusting covariates (iVAC). iVAC is a toolbox for Statistical Parametric Mapping 12 software (SPM12), which calculates the deviation from the normal range as a Z-score after adjusting for any covariates such as age, sex, and TIV (<https://amrc.iwate-med.ac.jp/en/project-2/download/>). iVAC provides whole brain- and ROI-based VBM results in individual patients in comparison with healthy control (HC) dataset. The aims of this study were 1) to investigate the characteristic findings of iVAC, 2) to compare iVAC findings and classic diagnostic hallmarks on MRI in patients with MSA, and 3) to elucidate the utility of iVAC for differentiating MSA from PD.

2. Methods

2.1. Characteristics and clinical evaluations of the participants

We recruited 53 patients with possible or probable MSA according to Gilman's criteria [1], consisting of 20 with MSA-Parkinsonism type (MSA-P) (11 males, 9 females) and 33 with MSA-Cerebellar type (MSA-C) (18 males, 15 females) (Table 1). All MSA patients underwent the evaluation of the Unified Multiple System Atrophy Rating Scale (UMSARS) part II [16]. We also included 53 age- and sex-matched patients diagnosed with PD (25 males, 28 females) from our PD cohort study [17] (Table 1). T1-weighted images (T1-WI) from 189 healthy volunteers, aging 40–79 years old, were selected from our ongoing Brain and Mind Research Center Aging Cohort Study at Nagoya University [18]. We did not include participants in this study who showed asymptomatic cerebral infarction or hemorrhage, benign brain tumor, leptomeningeal cyst, cavum septum pellucidum, cavum vergae, motion artifacts, obvious brain atrophy, or white matter abnormalities characterized by hyperintense lesions in T2-weighted imaging (T2-WI) that were grade 2 or 3 based on the Fazekas hyperintensity rating system.

The study conformed to the Ethical Guidelines for Medical and Health Research Involving Human Subjects endorsed by the Japanese government and was approved by the Ethics Review Committee of Nagoya University Graduate School of Medicine. Written informed consent was obtained from all the participants.

Table 1
Demographics and clinical characteristics of the participants.

Group (n)	Age at examination	Sex (Male/Female)	Duration (Year)	Motor score	
				UMSARS	MDS-UPDRS
				PartII	PartIII
HC (189)	62.0 ± 10.1	86/103	N/A	N/A	N/A
PD (53)	65.0 ± 7.4	25/28	3.2 ± 1.4	N/A	26.7 ± 14.5
MSA total (53)	63.0 ± 7.9	29/24	2.7 ± 1.4	20.7 ± 8.1	N/A
MSA-C (33)	63.8 ± 7.2	18/15	2.9 ± 1.4	17.8 ± 6.2*	N/A
MSA-P (20)	61.8 ± 8.8	11/9	2.5 ± 1.5	25.6 ± 8.6	N/A

HC: healthy controls, MSA: Multiple System Atrophy, MSA-P: Multiple System Atrophy-Parkinsonism type, MSA-C: Multiple System Atrophy-Cerebellar type. PD: Parkinson's disease, UMSARS: Unified Multiple System Atrophy Rating Scale, MDS-UPDRS: Movement Disorders Society-Unified Parkinson's Disease Rating Scale, N/A: Not Applicable.

*MSA-C vs MSA-P $p < 0.001$.

2.2. MRI acquisition protocol

All participants were scanned at the Brain and Mind Research Center, Nagoya University, using a Siemens Magnetom Verio (Siemens, Erlanger, Germany) 3.0-T scanner with a 32-channel head coil. T1-WI was acquired using a 3D Magnetization Prepared Rapid Acquisition Gradient Echo (MPRAGE) pulse sequence with the following parameters: repetition time (TR)/MPRAGE repetition time = April 7, 2500 m s, echo time (TE) = 2.48 m s, inversion time (TI) = 900 m s, 192 sagittal slices with a distance factor of 50% and 1-mm thickness, FOV = 256 mm, matrix dimension = 256 × 256, in-plane voxel resolution = 1.0 × 1.0 mm², flip angle (FA) = 8°, and total scan time = 5 min 49 s. T2-WI was acquired with the following parameters: TR = 5000 m s, TE = 82 m s, FA = 145°, 24 axial slices with a distance factor of 20% and 5-mm thickness, FOV = 220 mm, and matrix size = 193 × 256.

2.3. Image preprocessing

All images were preprocessed using the pipeline implemented in the Computational Anatomy Toolbox for SPM12 (CAT12; <http://www.neuro.uni-jena.de/cat/>, SPM12; <https://www.fl.ion.ucl.ac.uk/spm/software/spm12/>) running on MATLAB (R2016a; MathWorks, Natick, MA, USA). In the CAT12 toolbox, T1-WI was segmented into gray matter (GM), white matter (WM), and cerebrospinal fluid (CSF). The segmented images were normalized to the Montreal Neurological Institute (MNI) space using the Diffeomorphic Anatomical Registration Through Exponentiated Lie Algebra (DARTEL) algorithm [19]. The normalized images were then resampled to an isotropic voxel resolution of 1.5 × 1.5 × 1.5 mm³. The resulting images were smoothed using an 8-mm full-width-at-half-maximum 3-dimensional Gaussian filter using SPM12.

2.4. iVAC protocol

We used a multiple regression model for individual analysis. In a general linear model form, a voxel value of subject i , y_i , is expressed as:

$$y_i = \beta_0 + x_{i1}\beta_1 + x_{i2}\beta_2 + \dots + x_{iK}\beta_K + \varepsilon_i$$

where x_{ik} is the k th explanatory variables ($k = 1, \dots, K$; e.g., age, sex) for each subject i , β_k is the k th regression coefficient, while β_0 is a constant that is expressed as the intercept. ε_i is the error term with independent and identical normal distribution with zero-mean and variance σ^2 . This equation can be written in matrix form as:

$$\mathbf{y} = \mathbf{X}\boldsymbol{\beta} + \boldsymbol{\varepsilon}$$

where \mathbf{y} represents a column vector of voxel values with elements y_i , and \mathbf{X} is a matrix comprised of a column of ones for the constant terms β_0 and explanatory variables x_{ik} . $\boldsymbol{\beta}$ is the coefficient matrix with elements β_0 and β_k ($k = 1, \dots, K$), and $\boldsymbol{\varepsilon}$ is the error term vector having elements ε_i . The least square estimates of $\boldsymbol{\beta}$, $\hat{\boldsymbol{\beta}}$, is estimated using healthy control data as:

$$\hat{\boldsymbol{\beta}} = (\mathbf{X}'\mathbf{X})^{-1}\mathbf{X}'\mathbf{y}$$

and the predicted voxel values of the same control subjects, $\hat{\mathbf{y}}_{\text{ref}}$, were calculated as:

$$\hat{\mathbf{y}}_{\text{ref}} = \mathbf{X}\hat{\boldsymbol{\beta}}$$

the variance of the error ε , $\hat{\sigma}^2$, is then estimated as:

$$\hat{\sigma}^2 = \frac{(\mathbf{y} - \hat{\mathbf{y}}_{\text{ref}})'(\mathbf{y} - \hat{\mathbf{y}}_{\text{ref}})}{n - K},$$

where n is the number of subjects, K is the number of explanatory

variables. To calculate each voxel's Z-score in individual analysis, the predicted voxel value for a target subject, \hat{y}_{target} , was subtracted by the observed voxel value, further divided by the standard error (S.E.) of \hat{y}_{target} . The above estimate $\hat{\beta}$ is used to predict the voxel value for the explanatory variables of a target subject $\mathbf{x}_{\text{target}}$ ($1, x_1, \dots, x_K$)^T of individual analysis:

$$\hat{y}_{\text{target}} = \mathbf{x}_{\text{target}} \hat{\beta}$$

The standard error of \hat{y}_{target} is estimated from prediction calculation formula:

$$\text{S.E.}(\hat{y}_{\text{target}}) = \hat{\sigma} \sqrt{1 + \mathbf{x}_{\text{target}} (\mathbf{X}'\mathbf{X})^{-1} \mathbf{x}_{\text{target}}'}$$

Finally, Z-score is calculated as follows:

$$Z = \frac{\hat{y}_{\text{target}} - y_{\text{target}}}{\text{S.E.}(\hat{y}_{\text{target}})}$$

where y_{target} is the observed voxel value of the target subject.

We included age, sex, and TIV of healthy controls as explanatory variables in the general linear model form described above [20]. We can visually recognize how the target area is atrophied according to a color gradation system, which ranged from a Z-score of 2–5 at each voxel in this study. Deep brain structures such as the basal ganglia, including the putamen, cerebral cortex, and cerebellum, were evaluated by referring to gray matter Z-score images, while brainstem structures were evaluated according to white matter Z-score images.

For Z-score analysis at each brain structural change in target ROIs, the Neuromorphometrics template (<http://www.neuromorphometrics.com/>), consisting of 207 ROIs was used. In addition, the Z-scores of GM and WM structures were calculated separately, based on the image preprocessing procedure. To analyze the brainstem further, we used the Johns Hopkins University WM atlas (Eve Atlas, https://github.com/muschellij2/Eve_Atlas), which contains detailed WM parcellation including

the brainstem. We used the adapted version of the MNI space for overlapping between the original T1-WI of the Eve Atlas. By the iVAC scheme, the degree of atrophy in the reference ROIs can be calculated statistically as the total Z-score at every voxel divided by the number of voxels included in the target ROI (Z-score^{ROI}).

2.5. Evaluation of iVAC images and conventional brain MRI

We designated the abnormal findings on iVAC in patients with MSA as follows: 1) atrophy of the pons/MCP-positive (PoM-P): significant increase of the Z-score (>2) in the voxel value level that extended diffusely in the pons and MCP (Fig. 1 B-1 and C-1) 2) putaminal signal abnormality-positive (Put-P): significant increase of Z-score^{ROI} (>2) corresponding to the putamen at least on one side that included the dorsolateral part (Fig. 1–2 B-1). If there was an abnormal finding at least in 1) or 2), we defined it as significant. Of note, we designated the insignificant findings as follows: 1) limited increased Z-scores in the pons, MCP, or cerebellum (Supplementary Fig. 1A-1); and 2) even for a Z-score^{ROI} >2 on the putamen, if putaminal atrophy was consecutive with close structures, such as the insular or cerebral cortex, we did not regard it as a significant finding. In other words, putaminal atrophy should exist isolated from close structures (Supplementary Fig. 1B-1).

For T2-WI, two independent raters evaluated T2-WI of MSA and PD patients in a blinded manner, focusing on the occurrence of atrophy in the putamen and pons. Consensus on the results was discussed among both raters when conflicting results were found.

2.6. Statistical analysis

The results are expressed as the mean \pm standard deviation. To compare the MSA-P, MSA-C, PD, and HC groups, one-way analysis of variance or the Kruskal-Wallis test was used appropriately for analysis of age at MRI scanning. For analysis of the duration of illness and UMSARS score between MSA-C and MSA-P, an unpaired *t*-test or Mann-Whitney *U* test was used. The sex difference ratio among the groups was evaluated using Fisher's exact test. Statistical significance was set at $p < 0.05$.

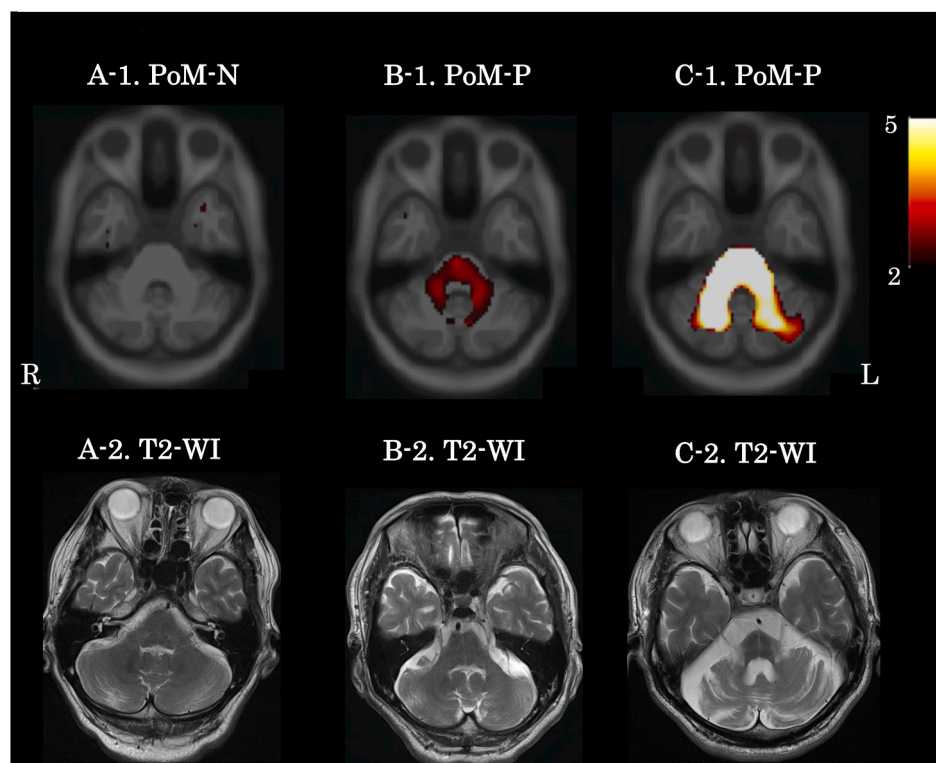


Fig. 1a. 1Evaluation of individual voxel-based morphometry with adjusting covariates (iVAC) images and T2-weighted imaging (WI) on the pons

The iVAC images are displayed in the upper row. A-1 shows no pontine atrophy (PoM-N), which is regarded as an insignificant finding. B-1 and C-1 show pontine and middle cerebellar peduncle (MCP) atrophy, which are both regarded as significant findings (PoM-P). Corresponding T2-WI scans are displayed in the lower row, of which A-2 and B-2 are evaluated visually as having no abnormalities.

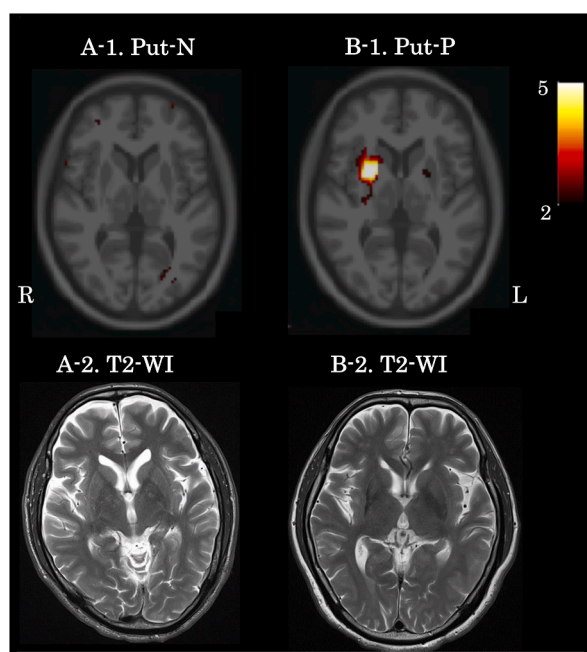


Fig. 1b. Evaluation of individual voxel-based morphometry with adjusting covariates (iVAC) images and T2-weighted imaging (WI) on the putamen. The iVAC images are displayed in the upper row. A-1 shows no putaminal atrophy (Put-N), which is regarded as an insignificant finding. B-1 shows right putaminal atrophy (Put-P). B-1 shows atrophy in the right dorsolateral putamen (Put-P), with Z-scores > 2 in the region of interest. Corresponding T2-WI scans are displayed in the lower row; A-2 shows no putaminal atrophy, while B-2 demonstrates right dorsolateral putaminal atrophy.

Sensitivity, specificity, positive predictive value, and negative predictive value were calculated to examine a diagnostic accuracy. The κ coefficient was calculated for the concordance ratio among the two independent raters for the iVAC images and T2-WI. Statistical analysis was performed in PASW Statistics 18.0 for Windows using SPSS version 24 (SPSS, Inc., Chicago, IL, USA).

3. Results

3.1. Demographics and clinical characteristics of the participants

Table 1 shows the clinical characteristics of the MSA-P, MSA-C, and PD patients. There were no significant differences in disease duration and age at examination between the MSA-P, MSA-C, and PD groups. The UMSARS part II scores were higher in patients with MSA-P than in those with MSA-C ($p < 0.001$).

3.2. Frequencies of MRI abnormalities in MSA and PD patients using iVAC

The κ coefficient among the two raters for the iVAC images and T2-WI was 0.979 and 0.895, respectively, and both were classified as excellent. Table 2 shows the frequencies of abnormal findings of the iVAC images in patients with MSA and PD. Of the patients with MSA, 98.1% showed significant atrophic changes (PoM-P or Put-P) on the iVAC images, but they were observed in only 3.8% of PD patients. As for clinical phenotype, 100% of MSA-C patients had PoM-P or Put-P and 84.8% of those showed only PoM-P. Of the MSA-P patients, 95% also had PoM-P or Put-P. Two of 53 PD patients had Put-P, but no patient was PoM-P.

Table 2

Frequencies of abnormal findings of the iVAC images in patients with MSA and PD.

Group	Pons/Putamen (n)				
	PoM-P or Put-P	PoM-P and Put-N	PoM-P and Put-P	PoM-N and Put-P	PoM-N and Put-N
MSA	52/53	32/53	19/53	1/53	1/53
total	(98.1%)	(60.4%)	(35.8%)	(1.9%)	(1.9%)
MSA-C	33/33	28/33	5/33	0/33	0/33
	(100.0%)	(84.8%)	(15.2%)	(0.0%)	(0.0%)
MSA-P	19/20	3/20	15/20	1/20	1/20
	(95.0%)	(15.0%)	(75.0%)	(5.0%)	(5.0%)
PD	2/53	0/53 (0%)	0/53 (0%)	2/53	51/53
	(3.8%)			(3.8%)	(96.2%)

iVAC: individual Voxel-Based Morphometry Adjusting Covariates, MSA: Multiple System Atrophy, MSA-C: Multiple System Atrophy-Cerebellar type, MSA-P: Multiple System Atrophy-Parkinsonism type, PD: Parkinson's disease.

PoM-P: Pons/Middle cerebellar peduncle-Positive, PoM-N: Pons/Middle cerebellar peduncle-Negative, Put-P: Putamen-Positive, Put-N: Putamen-Negative.

3.3. Comparison of iVAC and T2-WI findings in MSA and PD patients

Regarding the pons/MCP, 96.2% of MSA patients showed PoM-P on iVAC, but 60.4% of those had signal abnormalities on T2-WI in the pons/MCP (Supplementary Table 1). Particularly, in patients with MSA-C, significant atrophic changes were observed in 100% of patients on iVAC, but signal changes were detected in 66.7% of patients on T2-WI. No PD patient showed any abnormalities on iVAC images or T2-WI. In the putamen, the occurrence of signal abnormalities increased from 30% on T2-WI to 80% on iVAC in patients with MSA-P. Two of 53 PD patients showed signal changes on iVAC and T2-WI.

3.4. Ability of iVAC to differentiate between MSA-P and PD

As shown in Table 3, for the differentiation of MSA-P from PD, iVAC showed higher sensitivity (95.0% vs. 70.0%), positive predictive value (90.5% vs. 87.5%), and negative predictive value (98.1% vs. 89.5%) than T2-WI. Moreover, iVAC and T2-WI showed high specificity of 96.2%.

4. Discussion

This study demonstrated that iVAC was more sensitive and relevant than T2-WI for individual diagnostic purposes in patients with MSA. Using our definition of abnormal iVAC findings in the putamen and pons/MCP, all but one of 52 MSA patients and only 2 of 53 PD patients showed significant atrophic changes in the putamen or pons/MCP on iVAC. Regarding the differentiation of MSA-P from PD, the sensitivity and specificity of iVAC was 95% and 96.2%, respectively.

Recently, machine learning and deep learning techniques have been incorporated into various imaging techniques. These procedures

Table 3

Sensitivity, Specificity, PPV and NPV in MSA and PD between the iVAC and T2-WI.

Group	Sensitivity (%)		Specificity (%)		PPV (%)		NPV (%)	
	iVAC	T2	iVAC	T2	iVAC	T2	iVAC	T2
MSA vs PD	98.1	69.8	96.2	96.2	96.3	94.9	98.1	76.1
MSA-C vs PD	100	69.7	96.2	96.2	94.3	92	100	83.6
MSA-P vs PD	95	70	96.2	96.2	90.5	87.5	98.1	89.5

PPV: Positive Predictive Value, NPV: Negative Predictive Value, MSA: Multiple System Atrophy, iVAC: individual Voxel-Based Morphometry Adjusting Covariates, T2-WI: T2 Weighted Image, MSA-P: Multiple System Atrophy-Parkinsonism type, MSA-C: Multiple System Atrophy-Cerebellar type, PD: Parkinson's disease.

automate various analysis processes and provide highly accurate results, but since machines can learn from vast amounts of data by themselves and derive answers “autonomously,” researchers are unable to understand the actual process (i.e., the “black box” problem). A study using machine learning algorithms showed that the performance for the classification of PD–MSA-P and MSA-C–MSA-P was limited (balanced accuracy: 0.765–0.784; area under the receiver operating characteristic curve: 0.839–0.871) [21]. However, recent studies have shown high diagnostic accuracy for differentiating PD from MSA or progressive supranuclear using automated subcortical volume segmentation with FreeSurfer, resulting in diagnostic accuracy of 90% and specificity of 100% [11,12]. Conversely, iVAC successfully provided objective voxels and ROI Z-score information in a visible form. Thus, we could incorporate the characteristic pathological distribution patterns in the putamen and pons/MCP of MSA patients to define the abnormal findings in this study. On the basis of our experience, careful exclusion of non-specific atrophic changes in the putamen and brainstem is essential to reduce the misdiagnosis of MSA. We believe that a verifiable individual analysis system that can validate the process and the combination of novel computer technology, such as artificial intelligence, and accumulated knowledge is expected to improve the accuracy of MSA diagnosis. Although we did not perform direct comparisons of diagnostic accuracy with other methods such as the automated approaches described above, further studies will shed light on the differential potentials and utilities of both approaches.

In this study, the ratio of abnormal signals in the pons/MCP was also higher in MSA-P. Although MSA-C has a higher prevalence in Japan [22,23], the pons, MCP, and cerebellum may be more susceptible to impairment across Japanese patients with MSA. Conversely, the presence of abnormal findings in the putamen observed in MSA-P was also increased from 30% in T2-WI to 80% in iVAC, suggesting that iVAC could significantly improve the detection of abnormal atrophic changes in MSA, regardless of race. Further international collaborative studies will be needed to clarify this point.

VBM has been applied in many studies to investigate structural alterations in neurodegenerative disorders [8,9]. The Voxel-based Specific Regional Analysis system for Alzheimer’s Disease (VSRAD) [24] is also available for detecting individual hippocampal atrophy in daily clinical practice. VSRAD, similar to iVAC, calculates the standard deviation of each individual based on an HC dataset, regardless of covariates such as age, sex, and TIV that are thought to be influenced by individual analysis. However, supposed covariates are not adjusted appropriately, and more complicated stratification of covariates is required. By contrast, an advantage of iVAC is that it includes these covariates in the regression equation and thus statistically enables calculation in individual subjects. Additionally, the images obtained from iVAC are intuitively understandable. Our results using iVAC were superior to those from macroscopic evaluations with T2-WI, which was in agreement with a previous study showing that MRI findings precede the clinical diagnosis of MSA [3]. Moreover, considering the different atrophy patterns between MSA-C and MSA-P, our results might be consistent with the pathological hypothesis of MSA [25]. Therefore, as iVAC enables us to identify slight atrophy, which is difficult to detect with conventional brain MRI, it will be helpful for the analysis of the pathogenesis of MSA.

There are several limitations in this study. First, we did not examine spinocerebellar ataxia (SCA). Some kinds of SCA show similar neuroimaging features as MSA-C [26,27], while also mimicking MSA-P [28,29]. In addition, we did not investigate other parkinsonian syndromes such as progressive supranuclear palsy and corticobasal syndrome. Second, the reproducibility of these results in multiple centers and with different MRI acquisition protocols and the validation of HCs should be discussed carefully. Third, there was no neuropathological confirmation of MSA and PD.

5. Conclusions

We demonstrated the value of iVAC, a new quantitative VBM approach for individual patients. Importantly, it enabled us to recognize the morphological characteristics of MSA visually and with high accuracy. As such, it may represent a novel diagnostic screening tool for MSA.

Funding

This work was supported by Japan Society for the Promotion of Science (JSPS) KAKENHI Grant Number JP19K17030; This work was supported by Grants-in-Aid from the Research Committee of Central Nervous System Degenerative Diseases by the Ministry of Health, Labour, and Welfare and from the Integrated Research on Neuropsychiatric Disorders project carried out under the Strategic Research for Brain Sciences by the Ministry of Education, Culture, Sports, Science, and Technology of Japan. This work was also supported by a Grant-in-Aid for Scientific Research from the Ministry of Education, Culture, Sports, Science, and Technology (MEXT) of Japan (grant number: 80569781), and a Grant-in-Aid for Scientific Research on Innovative Areas (Brain Protein Aging and Dementia Control) (grant number: 26117002) from MEXT.

Author statement

JE, KH, KK, HW and GS contributed to the conception and design of the study. JE, KH, KK, YY, TK, AO, MM, RO, DM, SM contributed to the acquisition of the data. JE, KH, KK and HW contributed analysis of data. JE, KH, KK, HW, MK, OK and GS contributed to the interpretation of the data. FY and AK developed individual voxel-based morphometry adjusting covariates (iVAC) used in the study. KK adapted iVAC analysis pipeline to use for the study. JE contributed to the draft of the article. JE, KH, KK, HW, FY, AK, MK and GS revised the manuscript critically for important intellectual content. All authors approved the final version of the manuscript.

Declaration of competing interest

None declared.

Appendix A. Supplementary data

Supplementary data to this article can be found online at <https://doi.org/10.1016/j.parkreldis.2021.07.025>.

References

- [1] S. Gilman, G.K. Wenning, P.A. Low, D.J. Brooks, C.J. Mathias, J.Q. Trojanowski, N. W. Wood, C. Colosimo, A. Dürr, C.J. Fowler, H. Kaufmann, T. Klockgether, A. Lees, W. Poewe, N. Quinn, T. Revesz, D. Robertson, P. Sandroni, K. Seppi, M. Vidailhet, Second consensus statement on the diagnosis of multiple system atrophy, *Neurology* 71 (2008) 670–676, <https://doi.org/10.1212/01.wnl.0000324625.00404.15>.
- [2] D.J. Brooks, K. Seppi, Neuroimaging Working Group on MSA, Proposed neuroimaging criteria for the diagnosis of multiple system atrophy, *Mov. Disord.* 24 (2009) 949–964, <https://doi.org/10.1002/mds.22413>.
- [3] T.A. Mestre, A. Gupta, A.E. Lang, MRI signs of multiple system atrophy preceding the clinical diagnosis: the case for an imaging-supported probable MSA diagnostic category, *J. Neurol. Neurosurg. Psychiatry* 87 (2016) 443–444, <https://doi.org/10.1136/jnnp-2014-309645>.
- [4] V. Chelban, M. Bocchetta, S. Hassanein, N.A. Haridy, H. Houlden, J.D. Rohrer, An update on advances in magnetic resonance imaging of multiple system atrophy, *J. Neurol.* 266 (2019) 1036–1045, <https://doi.org/10.1007/s00415-018-9121-3>.
- [5] B. Heim, F. Krismer, R. De Marzi, K. Seppi, Magnetic resonance imaging for the diagnosis of Parkinson’s disease, *J. Neural. Transm.* 124 (2017) 915–964, <https://doi.org/10.1007/s00702-017-1717-8>.
- [6] M.T. Pellecchia, I. Stankovic, A. Fanciulli, F. Krismer, W.G. Meissner, J.A. Palma, J. N. Panicker, K. Seppi, G.K. Wenning, Members of the movement disorder society multiple system atrophy study group, can autonomic testing and imaging contribute to the early diagnosis of multiple system atrophy? A systematic review

- and recommendations by the movement disorder society multiple system Atrophy study group, *Mov. Disord. Clin. Pract.* 7 (2020) 750–762, <https://doi.org/10.1002/mdc3.13052>.
- [7] J. Ashburner, K.J. Friston, Unified segmentation, *Neuroimage* 26 (2005) 839–851, <https://doi.org/10.1016/j.neuroimage.2005.02.018>.
- [8] K. Specht, M. Minnerop, M. Abele, J. Reul, U. Wüllner, T. Klockgether, In vivo voxel-based morphometry in multiple system atrophy of the cerebellar type, *Arch. Neurol.* 60 (2003) 1431–1435, <https://doi.org/10.1001/archneur.60.10.1431>.
- [9] C. Brenneis, K. Seppi, M.F. Schocke, J. Müller, E. Luginger, S. Bösch, W.N. Löscher, C. Büchel, W. Poewe, G.K. Wenning, Voxel-based morphometry detects cortical atrophy in the Parkinson variant of multiple system atrophy, *Mov. Disord.* 18 (2003) 1132–1138, <https://doi.org/10.1002/mds.10502>.
- [10] A. Hotter, R. Esterhammer, M.F.H. Schocke, K. Seppi, Potential of advanced MR imaging techniques in the differential diagnosis of parkinsonism, *Mov. Disord.* 24 (2009), <https://doi.org/10.1002/mds.22648>, Suppl 2 S711–720.
- [11] C. Scherfler, G. Göbel, C. Müller, M. Nocker, G.K. Wenning, M. Schocke, W. Poewe, K. Seppi, Diagnostic potential of automated subcortical volume segmentation in atypical parkinsonism, *Neurology* 86 (2016) 1242–1249, <https://doi.org/10.1212/WNL.0000000000002518>.
- [12] F. Krismer, K. Seppi, G. Göbel, R. Steiger, I. Zucal, S. Boesch, E.R. Gizewski, G. K. Wenning, W. Poewe, C. Scherfler, Morphometric MRI profiles of multiple system atrophy variants and implications for differential diagnosis, *Mov. Disord.* 34 (2019) 1041–1048, <https://doi.org/10.1002/mds.27669>.
- [13] S. Crowley, H. Huang, J. Tanner, Q. Zhao, N.A. Schwab, L. Hizel, D. Ramon, B. Brumback, M. Ding, C.C. Price, Considering total intracranial volume and other nuisance variables in brain voxel based morphometry in idiopathic PD, *Brain Imaging Behav* 12 (2018) 1–12, <https://doi.org/10.1007/s11682-017-9709-8>.
- [14] A. Batla, E. De Pablo-Fernandez, R. Erro, M. Reich, G. Calandra-Buonaura, P. Barbosa, B. Balint, H. Ling, S. Islam, P. Cortelli, J. Volkmann, N. Quinn, J. L. Holton, T.T. Warner, K.P. Bhatia, Young-onset multiple system atrophy: clinical and pathological features, *Mov. Disord.* 33 (2018) 1099–1107, <https://doi.org/10.1002/mds.27450>.
- [15] Y.H. Lee, T. Ando, J.J. Lee, M.S. Baek, C.H. Lyoo, S.J. Kim, M. Kim, J.W. Cho, Y. H. Sohn, M. Katsuno, H. Watanabe, M. Yoshida, P.H. Lee, Later-onset multiple system atrophy: a multicenter Asian study, *Mov. Disord.* 35 (2020) 1692–1693, <https://doi.org/10.1002/mds.28177>.
- [16] G.K. Wenning, F. Tison, K. Seppi, C. Sampaio, A. Diem, F. Yekhelef, I. Ghorayeb, F. Ory, M. Galitzky, T. Scaravilli, M. Bozi, C. Colosimo, S. Gilman, C.W. Shults, N. P. Quinn, O. Rascol, W. Poewe, Multiple system Atrophy study group, development and validation of the unified multiple system Atrophy rating Scale (UMSARS), *Mov. Disord.* 19 (2004) 1391–1402, <https://doi.org/10.1002/mds.20255>.
- [17] K. Kawabata, H. Watanabe, E. Bagarinao, R. Ohdake, K. Hara, A. Ogura, M. Masuda, T. Kato, T. Tsuboi, S. Maesawa, M. Katsuno, G. Sobue, Cerebello-basal ganglia connectivity fingerprints related to motor/cognitive performance in Parkinson's disease, *Park. Relat. Disord.* 80 (2020) 21–27, <https://doi.org/10.1016/j.parkreldis.2020.09.005>.
- [18] E. Bagarinao, H. Watanabe, S. Maesawa, D. Mori, K. Hara, K. Kawabata, N. Yoneyama, R. Ohdake, K. Imai, M. Masuda, T. Yokoi, A. Ogura, T. Wakabayashi, M. Kuzuya, N. Ozaki, M. Hoshiyama, H. Isoda, S. Naganawa, G. Sobue, An unbiased data-driven age-related structural brain parcellation for the identification of intrinsic brain volume changes over the adult lifespan, *Neuroimage* 169 (2018) 134–144, <https://doi.org/10.1016/j.neuroimage.2017.12.014>.
- [19] J. Ashburner, A fast diffeomorphic image registration algorithm, *Neuroimage* 38 (2007) 95–113, <https://doi.org/10.1016/j.neuroimage.2007.07.007>.
- [20] J. Barnes, G.R. Ridgway, J. Bartlett, S.M.D. Henley, M. Lehmann, N. Hobbs, M. J. Clarkson, D.G. MacManus, S. Ourselin, N.C. Fox, Head size, age and gender adjustment in MRI studies: a necessary nuisance? *Neuroimage* 53 (2010) 1244–1255, <https://doi.org/10.1016/j.neuroimage.2010.06.025>.
- [21] L. Chougar, J. Faouzi, N. Pyatigorskaya, L. Yahia-Cherif, R. Gaurav, E. Biondetti, M. Villotte, R. Valabrègue, J.C. Corvol, A. Brice, L.L. Mariani, F. Cormier, M. Vidailhet, G. Dupont, I. Piot, D. Grabli, C. Payan, O. Colliot, B. Degos, S. Lehéry, Automated categorization of parkinsonian syndromes using magnetic resonance imaging in a clinical setting, *Mov. Disord.* (2020), <https://doi.org/10.1002/mds.28348>, Online ahead of print.
- [22] H. Watanabe, Y. Saito, S. Terao, T. Ando, T. Kachi, E. Mukai, I. Aiba, Y. Abe, A. Tamakoshi, M. Doyu, M. Hirayama, G. Sobue, Progression and prognosis in multiple system atrophy: an analysis of 230 Japanese patients, *Brain* 125 (2002) 1070–1083, <https://doi.org/10.1093/brain/awf117>.
- [23] G.K. Wenning, F. Geser, F. Krismer, K. Seppi, S. Duerr, S. Boesch, M. Köllensperger, G. Goebel, K.P. Pfeiffer, P. Barone, M.T. Pellecchia, N.P. Quinn, V. Koukouni, C. J. Fowler, A. Schrag, C.J. Mathias, N. Giladi, T. Gurevich, E. Dupont, K. Ostergaard, C.F. Nilsson, H. Widner, W. Oertel, K.M. Eggert, A. Albanese, F. del Sorbo, E. Tolosa, A. Cardozo, G. Deuschl, H. Hellriegel, T. Klockgether, R. Dodel, C. Sampaio, M. Coelho, R. Djaldetti, E. Melamed, T. Gasser, C. Kamm, G. Meco, C. Colosimo, O. Rascol, W.G. Meissner, F. Tison, W. Poewe, European Multiple System Atrophy Study Group, the natural history of multiple system atrophy: a prospective European cohort study, *Lancet Neurol.* 12 (2013) 264–274, [https://doi.org/10.1016/S1474-4422\(12\)70327-7](https://doi.org/10.1016/S1474-4422(12)70327-7).
- [24] H. Matsuda, S. Mizumura, K. Nemoto, F. Yamashita, E. Imabayashi, N. Sato, T. Asada, Automatic voxel-based morphometry of structural MRI by SPM8 plus diffeomorphic anatomic registration through exponentiated lie algebra improves the diagnosis of probable Alzheimer Disease, *AJNR Am. J. Neuroradiol.* 33 (2012) 1109–1114, <https://doi.org/10.3174/ajnr.A2935>.
- [25] K.A. Jellinger, Neuropathology of multiple system atrophy: new thoughts about pathogenesis, *Mov. Disord.* 29 (2014) 1720–1741, <https://doi.org/10.1002/mds.26052>.
- [26] H.J. Kim, B.S. Jeon, J. Shin, W.W. Lee, H. Park, Y.J. Jung, G. Ehm, Should genetic testing for SCAs be included in the diagnostic workup for MSA? *Neurology* 83 (2014) 1733–1738, <https://doi.org/10.1212/WNL.0000000000000965>.
- [27] Y.C. Lee, C.S. Liu, H.M. Wu, P.S. Wang, M.H. Chang, B.W. Soong, The 'hot cross bun' sign in the patients with spinocerebellar ataxia, *Eur. J. Neurol.* 16 (2009) 513–516, <https://doi.org/10.1111/j.1468-1331.2008.02524.x>.
- [28] J.M. Kim, S. Hong, G.P. Kim, Y.J. Choi, Y.K. Kim, S.S. Park, S.E. Kim, B.S. Jeon, Importance of low-range CAG expansion and CAA interruption in SCA2 Parkinsonism, *Arch. Neurol.* 64 (2007) 1510–1518, <https://doi.org/10.1001/archneur.64.10.1510>.
- [29] J.Y. Yun, J.M. Kim, H.J. Kim, Y.E. Kim, B.S. Jeon, SCA6 presenting with young-onset parkinsonism without ataxia, *Mov. Disord.* 27 (2012) 1067–1068, <https://doi.org/10.1002/mds.24977>.